WORLD CONFERENCE ON TIMBER ENGINEERING 2025
BRISBANE, AUSTRALIA

Advancing Timber for the Future Built Environment

NONLINEAR MODELLING OF CLT DIAPHRAGM CONFIGURATIONS WITH DIFFERENT SPLINE CONNECTIONS

Sebastian T. Akanji[1], Della Thomas[2], Adam R. Phillips[3], Erica Fischer[4]

ABSTRACT: Steel-timber hybrid buildings are being used throughout the United States to address market demands for more sustainable construction methods at reduced costs and increased speed. To ensure robust performance of these hybrid structures, it is crucial to understand the in-plane behaviour of the floor diaphragm when subjected to lateral loads. This paper summarizes the results of an analysis of the behaviour of cross-laminated timber (CLT) diaphragms to monotonic loading and an investigation on the influence of panel-to-panel connection strength and stiffness on overall diaphragm deflection using finite element (FE) analysis. Three configurations of CLT panels across an 18.3 m x 36.6 m prototype diaphragm using two different methods of calculating panel-to-panel spline connection strength were studied. The nonlinear behaviour of the panel-to-panel connections was modeled using the MultiLinear Plastic nonlinear material property in SAP2000. The CLT panel configurations studied were panels spanning the short direction of the diaphragm, panels spanning the long direction of the diaphragm with joints aligned, and panels spanning the long direction of the diaphragm with joints staggered. The results obtained show that staggered panel-to-panel connections have the potential to reduce diaphragm deflection compared to panel joints being aligned, but may be more costly due to increased planning, a larger number of fasteners required, and a larger number of tension straps required than diaphragms with aligned connections.

KEYWORDS: CLT diaphragms, mass timber, steel, steel-timber hybrid, nonlinear modelling

1 – INTRODUCTION

Steel-timber hybrid buildings are becoming a popular system because they combine the environmental benefits and lightweight nature of mass timber with the strength and long-spanning capabilities of structural steel. Also, all the structural members in this system are prefabricated in a factory and mounted onsite, which can help increase the speed of construction and reduce cost [1]. When cross laminated timber (CLT) is used as the floor diaphragm in a steel building, there are two main categories of connections that are critical for the load transfer from the steel frame to the diaphragm and eventually to the lateral force resisting system. The first is the connection between the CLT panels and the steel members that they are supported by. The second is the panel-to-panel connections between the individual CLT panels. If the CLT panels are designed as the seismic diaphragm, the steel gravity framing should not contribute significantly to its load resistance. For this reason, this study focused on the behaviour of the CLT diaphragm separate from the steel framing beneath it but using a representative aspect ratio and span length common for steel framed buildings.

Based on discussions with U.S. practicing engineers, the most common panel-to-panel connections use a plywood, LVL, or metal spline that is screwed or nailed along panel edges to resist shear forces. Several experimental and numerical studies have been carried out on spline panel-to-panel connections [1, 2, 3, 4, 5] and data from some of those studies is presented later in this paper to validate the numerical model used in this study. Fahkrzarei et al. [6] modelled different configurations of CLT diaphragms with the panels in various orientations and with joints both aligned and staggered. They conducted a parametric study in which they loaded two groups of archetype diaphragms: the first group with panel length parallel to loading, and the second with panel length perpendicular to loading. Each group consisted of two diaphragms: one with staggered joints and the other with nonstaggered (aligned)

[1] Sebastian T. Akanji, Department of Civil & Environmental Engineering, Virginia Tech, Blacksburg, USA. stakanji@vt.edu

[2] Della Thomas, Department of Civil & Environmental Engineering, Virginia Tech, Blacksburg, USA. della@vt.edu

[3] Adam R. Phillips, Department of Civil & Environmental Engineering, Virginia Tech, Blacksburg, USA. arp12@vt.edu

[4] Erica Fischer, School of Civil and Construction Engineering, Oregon State University, Corvallis, United States, Erica.Fischer@oregonstate.edu

https://doi.org/10.52202/080513-0526

joints. The spline connections were given the same stiffness (screw size and spacing) as a different study conducted by Line et al. [7], which was also used to validate their models. Fahkrzarei et al. [6] found that for panels loaded parallel to span direction, the staggered configuration was less stiff than the aligned one, whereas when loading was perpendicular to span direction, staggered joints were much stiffer. Since joint staggering prevents slip, it forces more load to be resisted by the CLT panels themselves. Therefore, the staggered joint configuration of the diaphragm would be stiffer regardless of whether the load is parallel or perpendicular to panel length. However, Fahkrzarei et al. [6] did not address why the results of the analysis demonstrated that the staggered configuration when loaded parallel to panel length produced a stiffness less than when the joints were aligned, nor did they assess the economic viability of staggered versus aligned configurations of the CLT panel joints.

The goals of the study summarized within this paper were to (1) investigate the effects of panel configuration and panel-to-panel spline strength on the deflection of CLT diaphragms; (2) investigate the factors that cause staggered CLT panel-to-panel connection configurations loaded parallel to panel length to have less stiffness [6] than aligned joints; and (3) explore the economic viability of staggered CLT panel-to-panel connection configurations through tracking the number of fasteners and tension straps needed for each configuration, as more fasteners and straps require both more material costs and construction labour.

2 – MATERIALS AND METHODS

The diaphragms analysed in this study were 36.57 m (120 ft.) wide by 18.29 m (60 ft.) deep. The loading was applied to the long face of the diaphragm. The three panel configurations investigated were with the panels spanning in the short direction of the diaphragm (C1), Figure 1(a), the panels spanning in the long direction of the diaphragm with joints aligned (C2), Figure 1(b), and panels spanning in the short direction of the diaphragm with the joints parallel to the direction of load staggered (C3), Figure 1(c). Each individual CLT panel was assumed to a 5-ply panel with a maximum size of 18.29 m x 3.0 m (60 ft. x 10 ft.).

The analysis was conducted using finite element (FE) modelling in SAP2000 [8], using the MultiLinear Plastic material model to capture the nonlinear spline behaviour. The main components of the diaphragm implemented in the finite element (FE) model are shown in Fig. 1(a): zero-length elements (ZLE) (springs) were used to model tension straps and spline connections, and 5-ply CLT panels of thickness 17.5cm (6.375in.) were modelled as thin shell elements (more details in Section 2.4). All analysed models meet the minimum requirements of the AWC SPDWS [9].

The diaphragms were analysed using displacement-controlled pushover analysis to get their ultimate behaviour, and then displacements at force levels representing a design level earthquake (DE) and maximum considered earthquake (MCE) were calculated. Results from this study show that diaphragm deflection depends on spline connection stiffness, as discussed in Section 3.

2.1 SEISMIC DEMANDS

This section briefly describes the calculation of the seismic demands on the prototype diaphragm analysed in this study. To calculate realistic seismic demands, the prototype was assumed to be a 6-story building (Figure 2(a)) with design spectral acceleration of 1.0g, to represent the building being located in a high seismic region such as San Francisco, CA or Seattle, WA. The diaphragm demands, F_{px}, were computed based on Section 12.10.1 of ASCE 7-22 [10]. The importance factor (I_e) was taken as 1.0 and the response modification coefficient (R) was taken as 6, which corresponds to a steel special concentrically braced frame. Total seismic weight per floor was estimated to be 23.84 kN/m^2 (83 psf). The diaphragm forces (F_{px}) were calculated for each floor and are shown in *Table 1*. The maximum diaphragm force, corresponding to Level 6, was used as the demand in this study.

It is a common practice to idealize diaphragms as simply supported or cantilevered deep beams with lateral loads applied as uniformly distributed loads [11]. Figure 2(b) shows the diaphragms idealized as simply supported deep beam. This idealization is used to calculate the shear and moment on the diaphragm, shear along diaphragm splines, transverse shear along splines perpendicular to the loading direction, and chord forces in tension and compression.

Table 1. Diaphragm demands obtained for a 6-story prototype building

Level	$\boldsymbol{F_{px}}$, kN/m^2 (*ksf*)
6	1.080 (*0.0226*)
5	0.997 (*0.0208*)
4	0.913 (*0.0191*)
3	0.830 (*0.0173*)
2	0.795 (*0.0166*)
1	0.795 (*0.0166*)

In Fig. 2(b), $V(x)$ is the shear force function (in kN) representing the shear diagram from the applied distributed

 https://doi.org/10.52202/080513-0526

load, w. The distributed load caused by the seismic force, w (in kN/m), applied in the N-S direction was calculated by multiplying the diaphragm demand, F_{px} (in kN/m^2), by the diaphragm depth, D (in m). The seismic force, w, induces shear demands that vary linearly along the length of the panel, as shown in the shear diagram and function, $V(x)$, in Figure 2(b). In each spline in the N-S direction, a unit shear, $v(x)$ (in kN/m), is induced with magnitude depending on its location, x, from the edge of the diaphragm. Similarly, a spline in the E-W direction would experience a unit shear, $v(y)$, depending on its location, y, from the long edge (L) of the diaphragm using a transverse shear approximation.

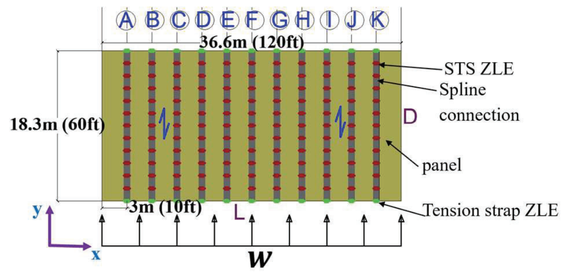

(a) Configuration 1 (C1) diaphragm

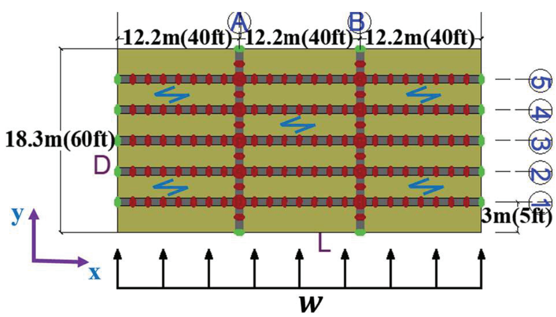

(b) Configuration 2 (C2) diaphragm

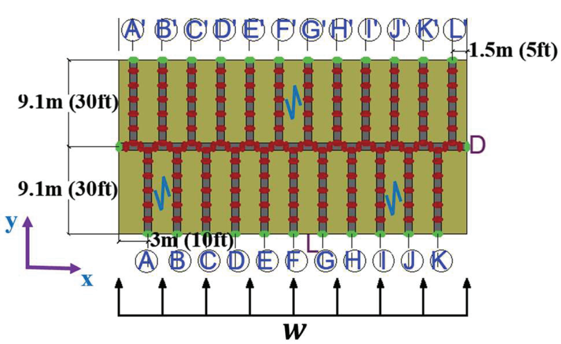

(c) Configuration 3 (C3) diaphragm

Figure 1. Diaphragm configurations modelled with screws (in red) and tension straps (in green) represented as ZLE (springs) at spline joints

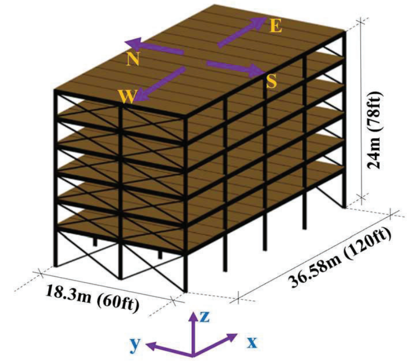

(a.) Isometric view

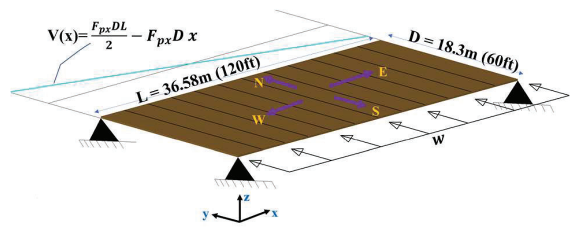

(b) Idealized simply supported diaphragm with distributed load and shear diagram

Figure 2. Prototype building used to compute diaphragm forces, and schematic diaphragm configuration

2.2 CAPACITY

Once demands at each spline location were calculated for the three configurations of panel layouts, the spline capacities needed to be calculated. For this study, it was assumed that the splines would be 19 mm (0.75 in.) Spruce-Pine-Fir (SPF) plywood fastened using 8 mm diameter mass timber screws. The screw capacities used were for MTC Solutions, ASSY 4.0 STS 8 mm screws. The design capacity per screw (Z) was controlled by Mode IIIs based on the specifications in the NDS [12]. The LRFD design capacity of the spline was calculated as 4.5 times Z times the phi-factor of 0.5, per the SDPWS [9] diaphragm design procedure to obtain an LRFD design capacity, Z', of 2509 N (564 lbs). The capacity per length of spline, $z(x)$, was then calculated by dividing Z' by the screw spacing, s. The tension straps were Simpson StrongTie MSTC40 of length 102 cm, width 7.6 cm, and thickness 1.4 mm with a tensile capacity of 20.5kN (4.6kips) [13].

2.3 PARAMETRIC CONFIGURATIONS

The spacing of the screws per spline was determined by setting capacity greater than demand at each spline location. Two screw spacing configurations were used for

https://doi.org/10.52202/080513-0526

this study. The first, called variable spacing (VS), tried to keep the demand to capacity ratio (DCR) as close to 1.0 as practical along every spline joint, resulting in different spacings for each spline depending on the spline locations. While this configuration may not be practical, it does represent the boundary of what meets the minimum code strength requirement. For the VS configuration, the screw spacing varied from 13 cm to 150 cm.

The second configuration, called same spacing (SS), used the highest demand spline to define the screw spacing for both vertical and horizontal splines in the diaphragm. This results in some splines being considerably over-designed but is preferable in practice due to the uniformity of spacing for screw installation and inspection. For the C1 panel layout the spacing was 28 cm, for the C2 panel layout the spacing was 74 cm, and for the C3 panel layout the spacing was 13 cm.

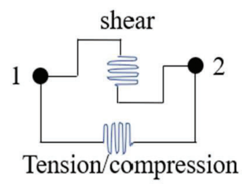

Figure 3. Typical ZLE with shear and axial capabilities

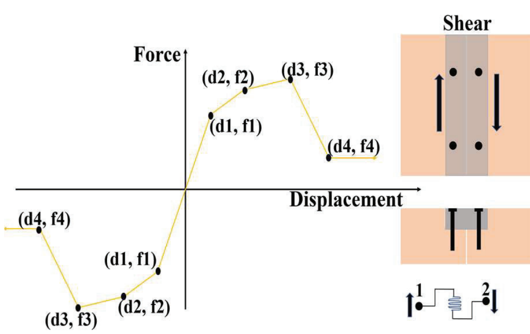

(a) Shear backbone curve

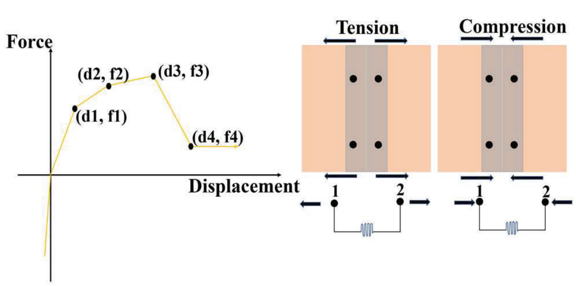

(b) Tension/compression backbone curve

Figure 4. Backbone parameters

2.4 FINITE ELEMENT (FE) MODELLING

The three configurations in Figure 1 were modelled in SAP2000 [8]. The STS spline connections and tension straps (depicted in Figure 1 (a)) were modelled using zero-length elements (ZLE) having shear and tension/compression capabilities and neglecting rotational behaviour [14, 15] (Fig 1). The spline ZLEs were applied every 1.5m (5ft), which is a tributary length representing a certain number of screws depending on the spacing. The CLT panels were modelled as quadrilateral thin shell elements with elastic and orthotropic behaviour. Figure 3 represents a typical ZLE connecting nodes 1 and 2 of two adjacent panels. The nonlinear behaviour of the spline connections was defined using a symmetric backbone curve with three ascending and one descending branches: represented by 8 pairs of force-displacement parameters for shear (Figure 4 (a)), and 4 pairs for tension (Figure 4 (b)). These piecewise linear backbone curves are identical to those used by Sun et al. [4] and Shen et al. [16] to model CLT connections. The backbone parameters were determined based on best fit to experimental data, as discussed in the subsequent section. Table 2 shows expressions that generate the data points in the backbone curves.

In Table 2, Z is the nominal dowel bearing capacity of a pair of screws; f1, f2, f3, f4, d1, d2, d3, and d4 are the backbone datapoints in Figure 4; k_1 is elastic stiffness for shear or tension obtained from Equation 1, proposed by Rodrigues et al. [11]; k_2, k_3, and k_4 are the stiffnesses of the piecewise inelastic parts of the backbone curve in Figure 4.

Table 2. Equations for backbone parameters

Parameter	Shear	Tension
f1	Z	Z
f2	1.7 f1	2.08 f1
f3	2.2 f1	2.52 f1
f4	1.77 f1	2.38 f1
k_1	Eq. 2	Eq. 2
k_2	0.184k_1	0.178k_1
k_3	0.0798k_1	0.0479k_1
k_4	-0.155k_1	-0.0241k_1
d1	f1/k_1	
d2	d1+ (f2- f1)/ k_2	
d3	d2+ (f3- f2)/ k_3	
d4	D3+ (f4- f3)/ k_4	

https://doi.org/10.52202/080513-0526

$$k_1 = \begin{cases} \frac{1}{2n}\gamma\, n_p; \ \text{shear} \\ \\ \frac{1}{4} n_p\, \gamma; \ \ \text{tension} \end{cases} \tag{1}$$

Where n is the number of screws in the direction perpendicular to spline length; n_p is the number of screws in a line of screws along spline length; γ is the slip modulus for dowel-type fasteners in wood-to-wood connections according to NDS [12].

2.4.1 Validation of backbone parameters

For compression, the compression test data from Wei et al. [17] for CLT loaded in-plane were used. The model ZLE procedure was validated against small-scale spline test data from Sun et al. [4] and Gavric et al. [5]. Both test data were based on the SOPHIE project conducted in Japan [5], where CLT spline connections consisted of a 180mm x 28mm LVL spline and 8mm diameter HBS screws of diameter 8mm with length 80mm spaced at 150mm. Fig. 6 shows a comparison of backbone curves from an experimental test that mimicked the SOPHIE project (Gavric et al. [5]), spline connection data from the said project used by Sun et al. [4] in their FE modelling of the connection described in this paragraph, and the backbone calibrated considering the spline connection characteristics of the SOPHIE project with the equations in Table 2. . The initial stiffness of the backbone curve using the equations in Table 2 closely matches the test data. The yield force is within 80% of the test data and ultimate strength is 20% greater than the tested data.

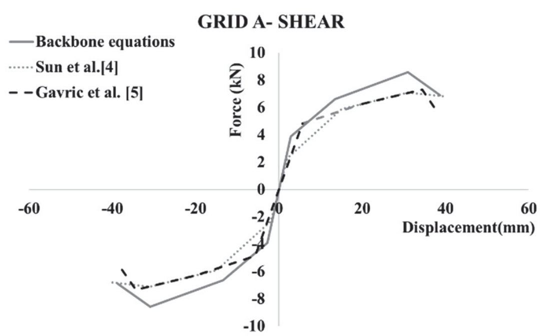

Figure 5. Benchmarked backbone equations vs test data

2.4.3 Validation of diaphragm modelling

To validate a full diaphragm model, the SAP2000 [8] model using the procedure described above was used to simulate the behaviour of a pair of diaphragms tested by Bhardwaj et al. [18] and the results were compared with those of the experiment. Bhardwaj et al. [18] tested two 6.1m (20ft) by 6.1m (20ft) cantilever CLT diaphragms, namely Diaphragm1 and Diaphragm2, supported by glulam beams, as shown in Figure 6. Both diaphragms used SPF plywood spline connections perpendicular to the direction of loading and were fixed to a rigid support using Simpson Strong-Tie hold-downs. Diaphragm1 was designed with a joint parallel to the direction of load at mid-span. The chord connection for this diaphragm had 5 tension straps at either end (Figure 6 (a)), while Diaphragm2 had continuous chords (Figure 6 (b)).

Pushover analysis was conducted on both diaphragms and the analysis results were compared with the test results. The target displacement 20cm (8in) was taken as the maximum displacement reached in the experiments. Figure 7(a) and Figure 7(b) show the total force vs total displacement plots and deformed shapes for Diaphragm1 and Diaphragm2, respectively. The behaviour of the test and the model followed a similar trend, though the model over-predicted stiffness by an average of 30%.

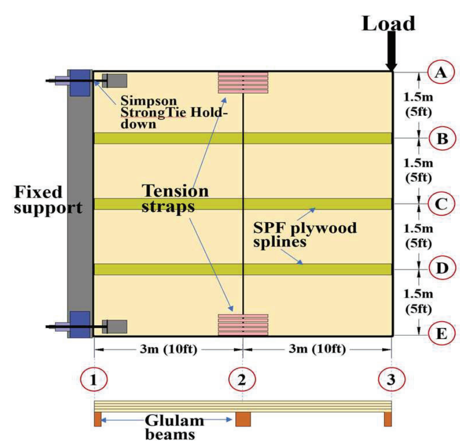

(a) *Diaphragm1*

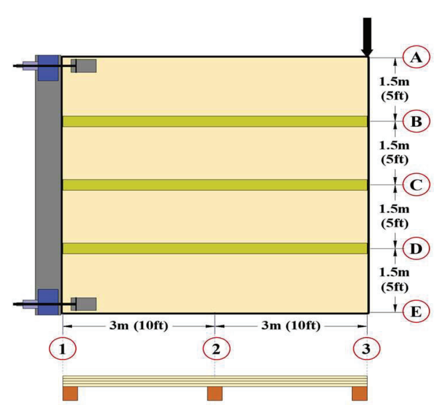

(b) *Diaphragm2*

Figure 6. Cantilever diaphragms tested by Bhardwaj et al. [16]

https://doi.org/10.52202/080513-0526

This could be attributed to the model not being able to capture some of the crushing observed in the tests, which may have caused a stiffness reduction, due to the inherent variability of wood as a material. The force carrying-capacity of the diaphragms per the test results was 185kN for Diaphragm1 and 164kN for Diaphragm2, whereas the corresponding capacities obtained from the models were 166kN and 172kN, representing an average error of 7%. Also, Figure 7 shows that the peak force was reached almost at the same displacement in both the test and model. This observation helped build confidence in the modelling narrative employed in this study.

Following the validation of the modelling process, the three diaphragm configurations (Fig. 1) were modelled.

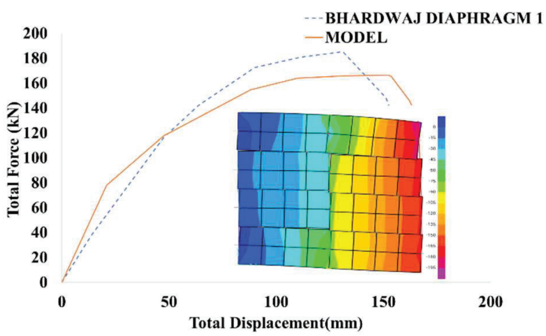

(a) *Diaphragm1 with vertical joint and tension straps*

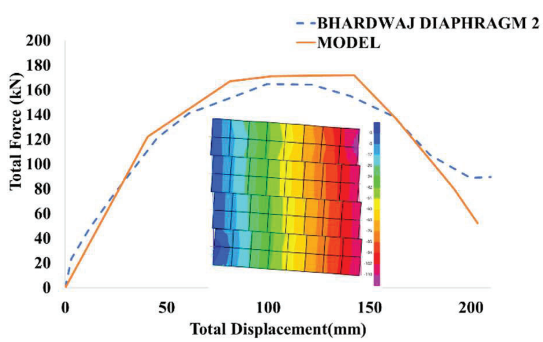

(b) *Diaphragm2 with no vertical joint*

Figure 7. Model validation results comparing SAP2000 model to experimental data by Bhardwaj et al. [18]

3 – RESULTS AND DISCUSSIONS

The results of the pushover analysis conducted for all three diaphragm configurations are presented in this section. First, their general behaviours are discussed, followed by a brief contrast between the configurations, and lastly, the economic and practical considerations for aligned versus staggered joints in CLT diaphragms.

Figure 8 shows the deflected shapes of the configurations and Figure 9 shows the plots of the pushover analysis results with DE and MCE force levels marked. In Figure 9, the plots with solid lines represent VS and dashed lines SS, and the additional dotted and dotted-dashed lines in Figure 9(b) represent two variations of C3 explained in subsequent paragraphs. The plots show that all three configurations had more than enough strength and stiffness to withstand the DE forces for which they were designed, and when loaded 1.5 times DE (MCE), the displacements remained within reasonable limits, ranging between 12mm and 35mm.

The results in Figure 9 reveal that the stiffness of the spline connections significantly affects overall diaphragm deformation. Also, it can be observed from the pushover force-displacement plots in Figure 9(a) that C1 and C2 exhibited inelastic behaviour as the aligned joints were free to slip in the direction of loading, as depicted in Figure 8(a) and Figure 8(b). This effect is more obvious in C1 where the stiffness and capacity increased significantly as the spacing type changed from VS to SS. This shows that C1 was more sensitive to spline connection stiffness than C2 since all spline connections were oriented in the loading direction, leading to more slip, and consequently more overall diaphragm deformation than C2. This aligns with the findings in Fakhrzarei et al. [6] as they also observed highest deformation in configurations with aligned joints.

Conversely, C3 remained linear (Figure 9(b)) because the staggered joints caused most of the shear force to be resisted by the panels, preventing joint slip and thus any possibility for inelastic behaviour of the diaphragm.

In Figure 9(a) for VS, C1 exhibited the largest displacement capacity of 400mm, which was double the maximum displacement reached in C2, and lower stiffness in the inelastic portion. For clarity in Figure 9, the displacement plots were stopped at 200mm. However, for SS, both diaphragms reached almost the same maximum displacement of about 185mm, this time C1 having higher stiffness than C2 due to the governing spacing in C1 being 28cm, and 74cm in C2, making the spline joints extremely rigid in the former. Both configurations reached approximately the same load capacity of about 3300kN. Figure 9(b) compares C1 with C3. For VS, C1 again exhibited almost four times more deformation than C3 (the plots C1-VS and C3-VS). Also, C3 exhibited lower capacity than C1 due to gap opening at staggered joints (Figure 8) (explained in detail in the next paragraph). For SS however, C3 exhibited both higher strength and stiffness because the governing spacing of 13cm increased the spline joint stiffness preventing gap opening.

https://doi.org/10.52202/080513-0526

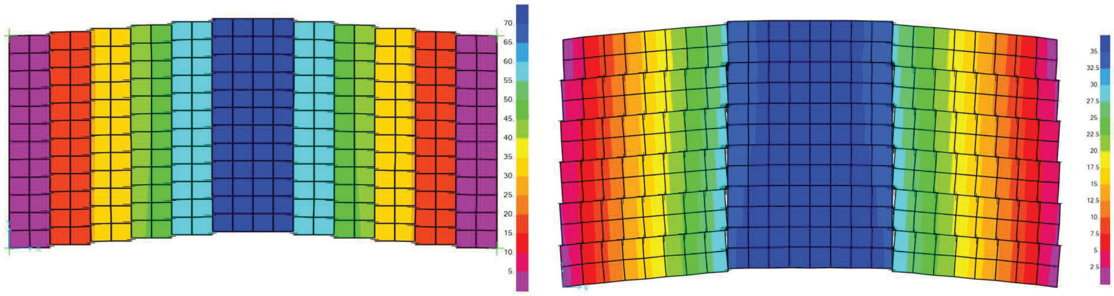

(a) C1: aligned spline joints, panels parallel to load *(b) C2: aligned spline joints, panels perpedicular to load*

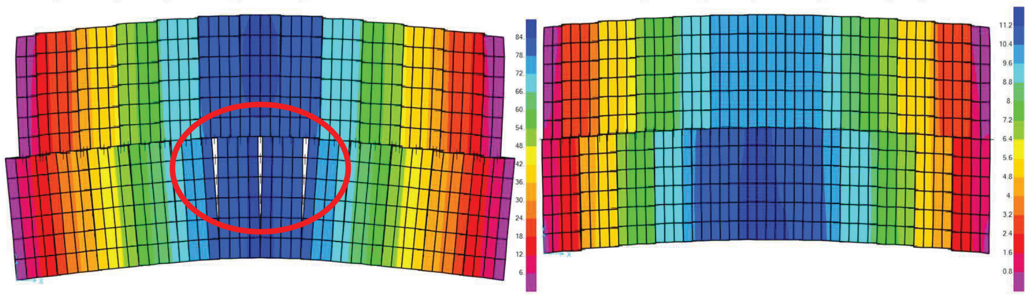

(c) C3-VS: staggered joints, panels parallel to load without straps at staggered joints *(d) C3-VS: staggered joints, panels parallel to load with straps at staggered joints*

Figure 8. Deflected shapes of all modelled configurations subjected to in-plane loading in the N-S direction

There is limited previous research on diaphragm configurations with staggered joints. For this reason, C3 is delved into with more detail. The deflected shapes of C3 are shown in Figure 8(c) and Figure 8(d). Figure 8(c) shows that this diaphragm behaved as two independent diaphragms with chord action at their ends. This led to wide gaps at the staggered joints as the diaphragm was subjected to in-plane flexure due to lateral load, causing significant slip in the W-E spline joint (perpendicular to load). The screws in N-S joints located beneath the W-E joint were thus subjected to both shear and tension forces. This violates the provisions in SDPWS [9] which states that connections designed to resist shear forces should not resist tension forces meant to be resisted by tension straps. Therefore, a variation of V3 was modelled with tension straps at the staggered joints, leading to the deflected shape in Figure 8(d). It is apparent from this deformed shape that the tension straps, while resisting the tension forces (and preventing gap opening), restored composite action of the diaphragm. The force-displacement behaviour of these two cases is shown in Figure 9(b) as C3-VS and C3-VS-STRAPS. The latter case with tension straps exhibited higher strength and stiffness. Another observation made was that when the governing screw spacing (SS) was used consistently in all spline connections in C3, the deflected shape was identical to that obtained for the case with straps at staggered joints (Figure 8(d)). The consistent spacing meant the spline joint in the W-E direction was much stiffer than the case with VS, which helped prevent gaps in the spline opening, depicted in the higher capacity and stiffness in the force-displacement plot in Figure 9(b) for C3-SS. This increased capacity and stiffness in C3-SS even without tension straps at staggered joints suggests that the previously described action in Figure 8(c) is mostly dependent on the stiffness of the spline connection in the W-E direction; the ability of this connection to slip and allow for gaps to open in the N-S joints located beneath the W-E joint. Nonetheless, to be code-compliant, it is recommended that tension straps be implemented at staggered joints so that any tension forces induced in that region be resisted by straps, not screws.

As mentioned in the introduction of this paper, Fakhrzarei et al. [6] concluded that for panels parallel to the direction of load, the diaphragm with aligned joints unexpectedly exhibited higher strength and stiffness than one with staggered joints. The findings of this study were similar, that staggering the joints did not increase strength and stiffness when tension straps were not included in the middle of the diaphragm. However, the results of this study showed that there are two main factors that affect the efficacy of staggered joints. First is the use of sufficient tension straps to resist net tension across the diaphragm, which may be at locations other than just the diaphragm chords. Second, if the tension strength of the splines is explicitly modelled, then a high number of screws in a spline generates a relatively large tension capacity, which helps keep tension gaps closed and increases stiffness of the overall diaphragm. This tension strength is not allowed to be accounted for in design codes, but it is present based on test data [4, 5]. The results of this study show that staggering joints when load is parallel to the panel length can result in large increases to strength and stiffness, so long as all tension forces are sufficiently resisted.

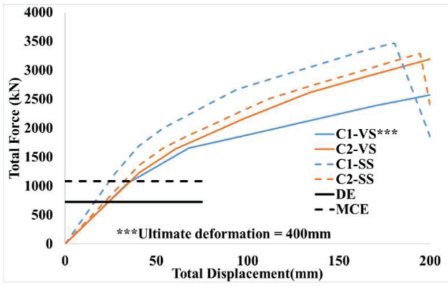

(a) C1 vs C2

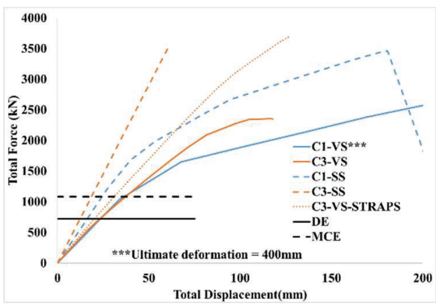

(b) C1 vs C3

Figure 9. Force vs displacement comparison of all configurations

This study also compared the diaphragm configurations based on the approximate cost to construct them. Since all the diaphragms used the same thickness and volume of CLT, it was assumed that price would be equivalent. Instead, the economic aspects were considered in terms of the number of screws and tension straps. Table 3 depicts the total number of screws for VS and SS configurations. It is obvious that in all cases of screw spacing, C3 requires the greatest number of screws, up to 6.5 times more than that of its counterparts. C2 requires the least number of screws. Similarly, C3 requires significantly more tension straps than the other configurations. More screws and tension straps likely result in higher cost of construction.

Table 3. Total number of screws and straps

Configuration	VS number of screws	SS number of screws	Number of straps
C1	792	1440	22
C2	444)	596	14
C3	1819	3888	48

4 – CONCLUSIONS

Three CLT diaphragm configurations – namely C1 with aligned spline connections and panels oriented parallel to load, C2 with aligned spline connections and panels oriented perpendicular to load, and C3 with staggered spline connections and panels oriented parallel to load – meant for CLT-steel hybrid systems were modelled via FE analysis in this study. The diaphragms were 36.6m (120ft) by 18.3m (60ft), which is an aspect ratio of 2:1. The spline connections, connected with self-tapping screws (STS), were modelled as zero length elements (ZLE) that incorporated the nonlinear characteristics of these STS connections from experimental data. Two screw configurations were designed for each diaphragm: varying spacing (VS), where each spline was designed with a screw spacing that resulted in a demand to capacity ratio of approximately 1.0 and same spacing (SS), where the screw spacing on every spline was the same as the most heavily loaded spline.

The results from this study show that all three configurations had enough strength and stiffness to resist the lateral DE and MCE forces applied with not more than 35mm of displacement. While C1 and C2 exhibited minor inelastic behaviour due to the spline joints being aligned, C3 was elastic when mid-diaphragm tension straps were used because slip was prevented at the staggered joints.

The results showed a significant reduction in deformation and increase in stiffness of the diaphragms as the spacing was changed from VS to SS. This indicates the importance of spline stiffness in CLT diaphragms especially when the joints are aligned. C1 exhibited the highest inelastic behaviour and up to 4 times more deformation capacity for VS. However, for SS, the stiffness and deformation depended on the governing screw spacing that was used.

Additionally, the number of screws required for C3 was two - three times more than required for C1 and C2, respectively. Consequently, the additional tension straps at staggered joints plus the large number of screws needed for C3 makes it unlike to be competitive from a cost perspective. C2 required the least number of screws and was slightly stiffer than the C1 configuration for the SS screw spacing. Based on the results obtained in this study, configurations C2 and C1 with aligned joints are recommended in design. Additionally, while not completely necessary, designing the diaphragm with uniform screw spacing limits the number of splines that yield and increases diaphragm stiffness, which reduces diaphragm deflection at DE and MCE.

https://doi.org/10.52202/080513-0526

ACKNOWLEDGMENT

This research was funded by the Charles Pankow Foundation. Any opinions, findings, and conclusions or recommendations expressed in this material are those of the authors and do not necessarily reflect the views of the sponsors.

REFERENCES

[1] A. Hassanieh, H. R. Valipour, and M. A. Bradford, “Experimental and numerical study of steel-timber composite (STC) beams,” *J. Constr. Steel Res.*, vol. 122, pp. 367–378, Jul. 2016, doi: 10.1016/j.jcsr.2016.04.005.

[2] K. Sullivan, T. H. Miller, and R. Gupta, “Behavior of cross-laminated timber diaphragm connections with self-tapping screws,” *Eng. Struct.*, vol. 168, pp. 505–524, Aug. 2018, doi: 10.1016/j.engstruct.2018.04.094.

[3] C. Loss, M. Piazza, and R. Zandonini, “Connections for steel–timber hybrid prefabricated buildings. Part I: Experimental tests,” *Constr. Build. Mater.*, vol. 122, pp. 781–795, Sep. 2016, doi: 10.1016/j.conbuildmat.2015.12.002.

[4] X. Sun, M. He, Z. Li, and Z. Shu, “Performance evaluation of multi-storey cross-laminated timber structures under different earthquake hazard levels,” *J. Wood Sci.*, vol. 64, no. 1, pp. 23–39, Feb. 2018, doi: 10.1007/s10086-017-1667-7.

[5] I. Gavric, Fragiacomo, Massimo, and Ceccotti, Ario, “Strength and deformation characteristics of typical x-lam connections,” *World Conf. Timber Eng.*, 2012.

[6] M. Fakhrzarei, H. Daneshvar, and Y. H. Chui, “Numerical parametric study of cross-laminated timber diaphragms under in-plane loading,” *Constr. Build. Mater.*, vol. 429, p. 136387, May 2024, doi: 10.1016/j.conbuildmat.2024.136387.

[7] P. Line, S. Nyseth, and N. Waltz, “Full-Scale Cross-Laminated Timber Diaphragm Evaluation. I: Design and Full-Scale Diaphragm Testing,” *J. Struct. Eng.*, vol. 148, no. 5, p. 04022037, May 2022, doi: 10.1061/(ASCE)ST.1943-541X.0003308.

[8] CSI: Structural Analysis and Design, SAP2000 V25, Computers and Structures, Inc.

[9] AWC: Special Design Provisions for Wind and Seismic (SDPWS), American Wood Council, Leesburg, VA., 2021.

[10] ASCE 7: Minimum Design Loads and Associated Criteria for Buildings and Other Structures, American

[11] L. G. Rodrigues *et al.*, “Analytical and Numerical Models for Wind and Seismic Design and Assessment of Mass Timber Diaphragms,” *J. Struct. Eng.*, vol. 150, no. 2, p. 04023229, Feb. 2024, doi: 10.1061/JSENDH.STENG-12265.

Society of Civil Engineers, 2021. [12] “2018 NDS,” American Wood Council. Accessed: Feb. 04, 2025. [Online]. Available: https://awc.org/publications/2018-nds/

[13] Simson StrongTie, MSTC40 Tension Strap Properties. Accessed: Mar. 13, 2025. Available: https://www.strongtie.com/lateralconnectorstiesandstraps_coldformedsteelconstruction/mstc_strap/p/mstc

[14] G. Rinaldin, C. Amadio, and M. Fragiacomo, “A component approach for the hysteretic behaviour of connections in cross-laminated wooden structures,” *Earthq. Eng. Struct. Dyn.*, vol. 42, no. 13, pp. 2023–2042, Oct. 2013, doi: 10.1002/eqe.2310.

[15] L. Pozza, A. Saetta, M. Savoia, and D. Talledo, “Coupled axial-shear numerical model for CLT connections,” *Constr. Build. Mater.*, vol. 150, pp. 568–582, Sep. 2017, doi: 10.1016/j.conbuildmat.2017.05.141.

[16] Y.-L. Shen, J. Schneider, S. Tesfamariam, S. F. Stiemer, and Z.-G. Mu, “Hysteresis behavior of bracket connection in cross-laminated-timber shear walls,” *Constr. Build. Mater.*, vol. 48, pp. 980–991, Nov. 2013, doi: 10.1016/j.conbuildmat.2013.07.050.

[17] P. Wei, B. J. Wang, H. Li, L. Wang, S. Peng, and L. Zhang, “A comparative study of compression behaviors of cross-laminated timber and glued-laminated timber columns,” *Constr. Build. Mater.*, vol. 222, pp. 86–95, Oct. 2019, doi: 10.1016/j.conbuildmat.2019.06.139.

[18] B. Bhardwaj, W. Pang, M. Stoner, D. Rammer, and S. E. Pryor, “Experimental Characterization of Cantilever Cross-Laminated Timber Diaphragms under In-Plane Shear Load,” *J. Struct. Eng.*, vol. 150, no. 2, p. 04023220, Feb. 2024, doi: 10.1061/JSENDH.STENG-12590.